Clays and Clay Minerals, Vol. 60, No. 1, 18–31, 2012.

ORIGIN OF SAPONITE-RICH CLAYS IN A FOSSIL SERPENTINITE-HOSTED HYDROTHERMAL SYSTEM IN THE CRUSTAL BASEMENT OF THE HYBLEAN PLATEAU (SICILY, ITALY)

FABIO C. MANUELLA[1,*], SERAFINA CARBONE[1], AND GIOVANNI BARRECA[1]

Dipartimento di Scienze Biologiche, Geologiche e Ambientali, Università di Catania, Corso Italia 57, I-95129, Catania, Italy

Abstract—A diapiric intrusion of clays in the Carlentini Formation (Tortonian) was discovered in a quarry at S. Demetrio High (Hyblean Plateau, Sicily, Italy). Seven clay samples were analyzed by different analytical methods, including X-ray powder diffraction (XRD) and Fourier-transform infrared (FTIR) spectroscopy, to determine the composition and mechanism of formation (sedimentary *vs.* hydrothermal) of these clays. Ferric saponite, carbonates (calcite and traces of ankerite), quartz, pyrite, and zeolites (phillipsite and harmotome) were detected using XRD and FTIR. This mineral assemblage, dominated by Fe-rich saponite, and the abundance of light rare-earth elements (*LREE*), Eu, fluid-mobile elements (FME > 10 × primordial mantle: Li, Be, B, As, Sb, Pb, U, Ba, Sr, Cs), and other incompatible elements (Zr = 169 ppm, Nb = 46 ppm, Th = 11 ppm, on average) imply that S. Demetrio clays precipitated from a mixture of hot Si-rich hydrothermal fluids (350−400ºC) and cold seawater. The evidence is in accord with the affinity of clays for hydrothermally modified mafic and ultramafic rocks, forming the Hyblean lower crust, based on multi-element comparisons, and on the occurrence of trace amounts of chrysotile $2M_{c1}$ and sepiolite. The association of long-chain aliphatic-aromatic hydrocarbons (intensity ratios $I_{2927}/I_{2957} > 0.5$) with hydrothermal clays, the lack of fossils, and the similarity of the IR absorption bands with those of organic compounds detected previously in some metasomatized Hyblean gabbroic xenoliths suggest a possible abiogenic origin of hydrocarbons *via* a Fischer-Tropsch-type reaction. The S. Demetrio clay diapir was emplaced at shallow crustal levels in the Late Miocene as a consequence of the interaction, at a greater depth, of an uprising basalt magma and the products of an early, serpentinite-hosted hydrothermal system.

Abstract—Fischer-Tropsch-type Synthesis, Hyblean Plateau, Hydrocarbons, Hydrothermal System, Saponite, Sicily.

INTRODUCTION

A recent geological survey at the Iazzotto quarry (S. Demetrio High; Figure 1), in the northeastern sector of the Hyblean Plateau (Sicily, Italy), led to the discovery of hydrocarbon-bearing clays intruded diapirically in a diatremic tuff-breccia deposit, the Carlentini Formation (Tortonian; Carbone and Lentini, 1981), the presence of which was inferred previously by the S. Demetrio 1 Agip well (37º21′36N, 15º1′50E; maximum depth 1547.5 m.b.s.l.; Torelli *et al.*, 1998).

Organic-rich clays, generally referred to as black shales (or bituminous rocks), can form in different sedimentary settings (Emeis and Weissert, 2009), as well as by weathering of mafic and ultramafic lithologies (Dos Anjos *et al.*, 2010). In addition, sediments covering the hydrothermal field of Logatchev in the Mid-Atlantic Ridge (MAR), which contain abundant bituminous materials of abiogenic origin (Pikovskii *et al.*, 2004), consist mainly of Fe-smectites (Gablina *et al.*, 2006). These clay minerals represent the dominant mineral species in many hydrothermal systems (*e.g.* Mt. Saldanha – Dias and Barriga, 2006; TAG – Severmann *et al.*, 2004; Nimis *et al.*, 2004).

The present study reports mineralogical and geochemical data for S. Demetrio clays which may help to determine their origin and composition, as well as the physicochemical conditions existing at the time of their formation. In particular, two possible source types were considered for the S. Demetrio clays: (1) sedimentary, related to the occurrence in the Hyblean area of a mainly pelitic deposit known as the Streppenosa Formation (Hettangian−Sinermurian; Zappaterra, 1994; Bianchi *et al*., 1987); and (2) hydrothermal, like hydrocarbon-bearing clays found in some metasomatized oxide-rich gabbros (Ciliberto *et al*., 2009).

GEOLOGICAL SETTINGS

The Hyblean Plateau

The Hyblean Plateau in southeastern Sicily is usually interpreted as being an emerged portion of the Pelagian block (Ben-Avraham *et al*., 1990), which is characterized by a crustal thickness of 25−30 km (Scarascia *et al*., 2000), deduced from the interpretation of seismic profiles. The northeastern border of the Hyblean area is affected by two main fault systems, one extensional, trending NE−SW, which developed from the northward collapse of the Hyblean Plateau beneath the Maghrebian

* E-mail address of corresponding author:
fmanuella@alice.it
DOI: 10.1346/CCMN.2012.0600102

thrust belt, and a NNW–SSE trending oblique fault belt (the Hyblean-Malta Escarpment) which controls the eastern side of the Plateau separating this from the Ionian abyssal plain.

The nature of the Hyblean crustal basement was inferred from several deep-seated xenoliths (Scribano, 1986), which occur in the tuff-breccia deposits of some Upper Miocenic alkaline-mafic diatremes (Carbone and Lentini, 1981). The main lithologies are represented by spinel-lherzolites and harzburgites (Scribano, 1987), which exhibit chemical compositions and isotopic signatures consistent with a depleted mantle origin, minor sheared oxide-gabbros (Scribano *et al.*, 2006b), along with various sedimentary and volcanic rocks Meso–Cenozoic in age.

The Hyblean lower crust was suggested by Scribano *et al.* (2006b) to have formed from a fossil ultramafic core complex, which was exposed by tectonic means, on the seafloor of an early oceanic domain. Petrological investigations in some metasomatized gabbroic xenoliths suggested the existence of a fossil abyssal-type hydrothermal system (Scribano *et al.*, 2006a). Discovery of hydrothermal zircons in gabbroic xenoliths enabled dating (by *in situ* U-Pb analyses) of the hydrothermal system, and hence serpentinization, according to Dubińska *et al.* (2004), as Early Triassic (~246 Ma; Sapienza *et al.*, 2007). Detailed mineralogical study of serpentine veins in some partially serpentinized harzburgite xenoliths, exhibiting a degree of serpentinization up to 80% (by volume), led Manuella (2011) to suggest that peridotites were altered by the circulation of hypersaline aqueous fluids derived from seawater in the Hyblean basement, at a temperature of 350–400ºC and at a pressure of <0.2 GPa.

S. Demetrio High

The S. Demetrio ridge, in the northeastern sector of the Hyblean Plateau (Figure 1), is a NE–SW structural high made up of Neogene-Quaternary sedimentary and volcanic rocks. The exposed sequence consists, from the bottom, of Lower–Middle Miocene calcarenites and calcirudites of the Monti Climiti Formation (Grasso and Lentini, 1982), which are covered by Tortonian volcanoclastites (Carlentini Formation; Carbone and Lentini, 1981). On the southern slope of the S. Demetrio High, Late Tortonian–Early Messinian reefal to lagoonal limestones (Carrubba Formation, Grasso and Lentini, 1982) lie unconformably on the Carlentini Formation. Upward, black submarine Messinian nephelinitic lava flows (K/Ar date of 5.4 Ma; Behncke, 1999) occur.

Recent volcanic rocks, which are related to NE–SW extensional fault system (Grasso *et al.*, 2004) consist of alkaline volcanic products (S. Febronia Unit) ~1.4 Ma old (Trua *et al.*, 1997).

Recently, large-scale excavation (affecting an area of ~0.7 km^2) for the installation of a landfill site in the Iazzotto area (Figure 1) allowed examination of the stratigraphical successions and their geometrical relations. Three main lithostratigraphic units at the site were recognized, consisting, from the top, of lower Pleistocene calcarenites and basal conglomerates (A unit in Figure 2). A wide erosive surface separated these from

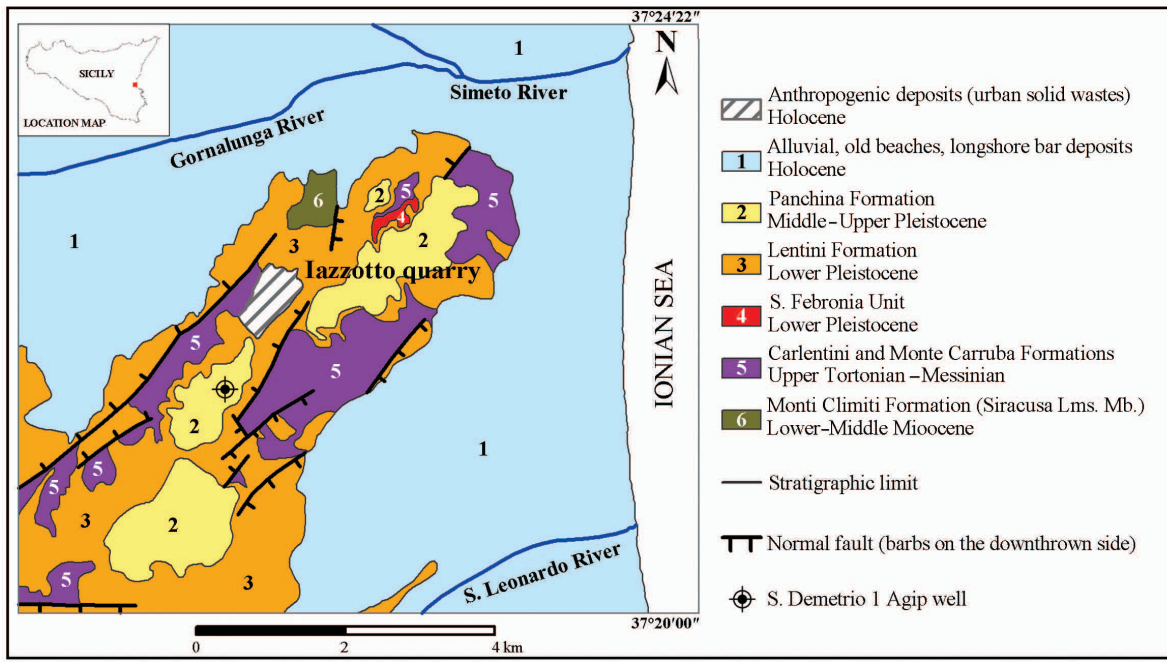

Figure 1. Geological map of S. Demetrio High. The field survey was performed by G. Sturiale and S. Carbone.

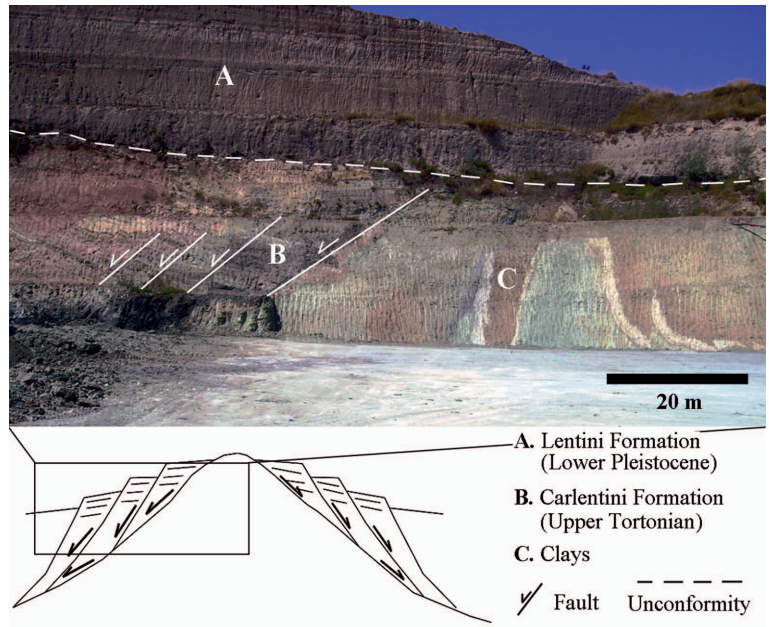

Figure 2. Diapiric intrusion of clays at the Iazzotto quarry, S. Demetrio High (southeastern Sicily, Italy).

the underlying Carlentini Formation (B unit in Figure 2) and clays (C unit in Figure 2). The internal structure observed in the C unit and its relationship to the B unit suggest that the emplacement of the clays was driven by a diapiric intrusion. In fact, a pervasive set of S-dipping low-angle normal faults, which affect the Carlentini Formation, was interpreted as flank-collapse structures related to the diapiric uprise (see inset in Figure 2).

ANALYTICAL METHODS

Seven clay samples, collected randomly from the intrusive body at the S. Demetrio High quarry, were investigated using a number of analytical techniques to determine their mineralogical and geochemical compositions. Each sample was dispersed in double-distilled water and ground gently in a ceramic mortar to extract coarse sediments (4−62.5 μm) by manual sieving. A mixture of fine sediments (<2 μm) and double-distilled water was centrifuged five times for 15 min at 750 rpm (corresponding to a g force of ~150 N) to separate the clay fraction. The residue was dried in an extractor hood at a temperature of 25ºC.

Clay-enriched samples were analyzed for clay mineral and coarse-grained phase compositions using a Siemens D5000 X-ray powder diffractometer at the Dipartimento di Scienze Geologiche di Catania (Italy), equipped with monochromatic CuKα radiation (wavelength = 1.5406 Å), a Ni filter, voltage = 40 kV, current = 30 mA, and slits of 2 mm, 1 mm, and 0.2 mm. Measurements were acquired as a continuous scan from 3 to 80º2θ, with a calculated step size of 0.020º2θ and a calculated time per step of 1.00 s. Clay samples were prepared as KBr pellets (1:100 ratio of sample/KBr) and then analyzed by FTIR at the Dipartimento di Scienze Chimiche di Catania (Italy) using a Jasco 430 spectrometer equipped with a Triglycine sulfate (TGS) detector, with a 2 cm^{-1} resolution over the range 4000−400 cm^{-1}.

Whole-rock geochemical data (Table 1) were obtained at the Dipartimento di Scienze Geologiche di Catania by X-ray fluorescence (XRF) with a Philips PW2404 WD-XRF on powder pellets with bulk sediments; XRF data were integrated with loss on ignition (L.O.I.). The amount of calcium carbonate (Cc) was calculated and then subtracted from major-element compositions:

$$CaO_{Cc}\ (wt.\%) = CaO_{(sample)} - [(56.84 \times P_2O_{5(sample)})/43.16] \quad (1)$$

Table 1. Mineral assemblages in S. Demetrio clays, as determined by X-ray powder diffraction analyses.

Samples	CSD 3	CSD 4	CSD 5	CSD 6	CSD 7	CSD 8	CSD 11
Saponite	■	■	■	■	■	■	■
Sepiolite						■	
Chrysotile			■		■		
Quartz	■			■	■		
Pyrite				■			
Phillipsite						■	
Harmotome						■	
Calcite		■	■	■	■	■	■
Ankerite				■	■		■

CO_{2Cc} (wt.%) = ($CaO_{Cc} \times 43.97$)/56.03 (2)

$CaCO_3$ (wt.%) = CaO_{Cc}+CO_{2Cc} (3)

The *REE* and other trace elements for samples CSD 3, CSD 7, and CSD 8 were measured at Activation Laboratories, Ltd. (Actilabs, Toronto, Canada) by Total Digestion-Inductively Coupled Plasma (TD-ICP) and Instrumental Neutron Activation Analysis (INAA). In addition, the concentrations of B and Li (detection limits of 0.5 ppm and 1 ppm, respectively) in all clay samples were determined at Actilabs by Prompt Gamma Neutron Activation Analysis (PGNAA) and TD-ICP, respectively. Detailed information on the aforementioned analytical methods can be found on the website www.actlabs.com.

RESULTS

Mineralogy and chemistry of the clays

XRD. Numerous crystalline phases (Table 1) were identified using XRD of randomly oriented powders. The XRD patterns of all samples exhibited characteristic peaks (Figure 3) of saponite (JCPDS card no. 29-1491), the basal reflection (d_{001}) of which is at 15.4 Å (5.726º2θ), followed by peaks at 4.52 Å (19.633º2θ) and 2.59 Å (34.623º2θ). The trioctahedral nature of the clay fraction was based on the d_{060} reflection at an average value of 1.54 Å (60.00º2θ), according to Grauby *et al.* (1994). Another clay mineral found was sepiolite (JCPDS card no. 13-595), which was identified in sample CSD 8 [12.2 Å (7.228º2θ); 2.56 Å (35.054º2θ); 4.32 Å (20.532º2θ); 3.75 Å (23.691º2θ); 2.28 Å (39.481º2θ)]. Trace amounts of chrysotile $2M_{c1}$ (JCPDS card no. 21-1262) were found in samples CSD 5 and CSD 7, according to peaks at 4.55 Å (19.500º2θ), 7.28 Å (12.142º2θ), 3.64 Å (24.414º2θ), 2.62 Å (34.193º2θ), and 2.55 Å (35.219º2θ), which are very similar to those detected in some partially serpentinized Hyblean peridotites (Manuella, 2011). The coarse-grained minerals consisted mainly of calcite [3.03 Å (29.435º2θ); 3.86 Å (23.060º2θ)], quartz [3.03 Å (29.435º2θ); 3.86 Å (23.060º2θ)], and traces of ankerite [2.904 Å (30.765º2θ); 2.206 Å (40.894º2θ)]. Pyrite (JCPDS card no. 42-1340) occurred only in sample CSD 6 as shown by peaks at 1.63 Å (56.250º2θ), 2.71 Å (33.026º2θ), 2.42 Å (37.066º2θ), 2.21 Å (40.757º2θ), and 3.13 Å (28.478º2θ). In addition, two zeolites were found in sample CSD 8: phillipsite [JCPDS no. 20-923; 3.20 Å (27.865º2θ), 7.19 Å (12.296º2θ); 6.437 Å (13.745º2θ)] and harmotome [JCPDS no. 39-1377; 3.20 Å (27.865º2θ); 7.19 Å (12.296º2θ); 6.437 Å (13.745º2θ)].

FTIR. The IR spectra of all the clay samples (Figure 4, Table 2) exhibited bands at 3676 and 3601 cm^{-1} attributed to (Mg, Fe^{3+})$_3$OH stretching vibrations (Farmer, 1974) in octahedral sites, and OH-stretching bands in interlayer sheets at 3562 cm^{-1}, as well as bending vibration of hygroscopic water at 3400 cm^{-1} (Parthasarathy *et al.*, 2003). These peaks reveal the presence of a trioctahedral smectite, probably a ferric saponite as supported by bands at 3601 and 3400 cm^{-1} (Parthasarathy *et al.*, 2003). Hydroxyl bending vibrations occurred at 3207 and 1600 cm^{-1} (Farmer, 1974; Brindley *et al.*, 1979) and libration modes of Mg_3OH groups at 694, 672, 656, and 590 cm^{-1} are characteristic features of trioctahedral smectites (Farmer, 1974; Brindley *et al.*, 1979; Benhammou *et al.*, 2009). The intense band at 1010 cm^{-1} and its shoulder at 1100 cm^{-1}, with two weak peaks at 780 and 770 cm^{-1}, were produced by stretching vibrations of Si–O bonds in tetrahedral sheets, and the band at 504 cm^{-1} was attributed to Si–O bending (Brindley *et al.*, 1979; Benhammou *et al.*, 2009). Finally, weak peaks occurred in the range 460–400 cm^{-1} attributed to stretching

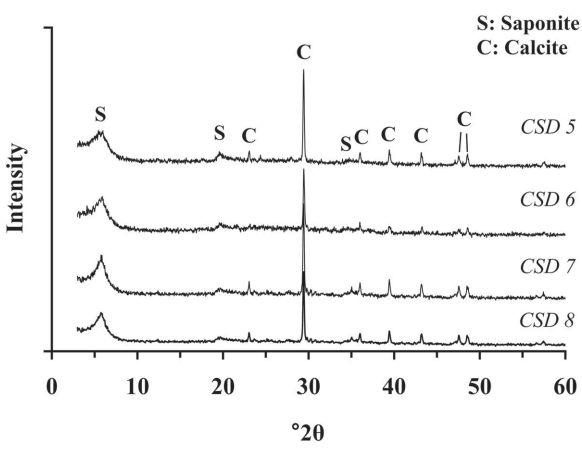

Figure 3. Powder XRD pattern of some clay samples in the range 3–60º2θ.

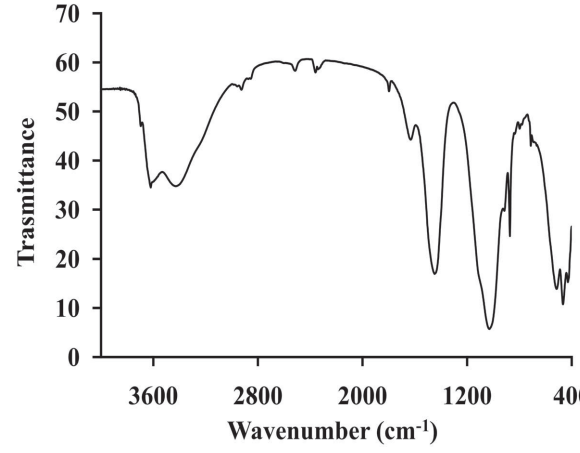

Figure 4. IR spectrum of a representative clay sample (CSD 7) in the range 4000–400 cm^{-1}.

Table 2. Interpretation of bands in IR spectra of S. Demetrio clays.

CSD 3	CSD 4	CSD 5	CSD 6	CSD 7	CSD 8	CSD 11	Interpretation	References
–	–	–	3678	3676	–	3679	$MgFe^{3+}OH$ str.	1
–	–	–	3601	3601	3601	3601	$MgFe^{3+}OH$ str.	1; 3
3560	3567	3551	3568	3562	3548	3550	H_2O str.	3
3405	3403	3406	3410	3408	3408	3404	H_2O str.	1; 3
3206	3213	3207	3197	3207	3209	3216	H_2O bend.	1
–	1790	1793	1773	1789	1773	1793	CO_3^{2-} comb.	5
1620	1617	1606	1618	1618	1625	1606	H_2O bend.	2
1418	1423	1427	1432	1431	1418	1425	CO_3^{2-} str.	5
1100	1083	1081	1102	1103	1107	1093	Si-O str.	2; 4
1015	1011	1011	1016	1010	1019	1009	Si-O str.	2; 4
909	884	907	908	908	910	909	Si-O-Mg str.	4
870	872	872	870	871	870	871	CO_3^{2-} str.	5
823	–	–	822	823	818	816	$Fe_2^{3+}OH$ libr.	1
780	–	–	777	781	788	776	Si-O str.	4
764	–	750	763	770	762	752	Si-O str.	4
736	710	710	724	720	729	710	CO_3^{2-} str.	5
–	–	–	697	694	697	–	$MgFe^{3+}OH$ libr.	2
–	–	–	668	672	673	–	$MgFe^{3+}OH$ libr., Si-O-Mg str.	2; 4
653	647	650	647	656	651	650	$MgFe^{3+}OH$ libr.	1; 4
–	586	–	–	–	584	594	$MgFe^{3+}OH$ libr.	4
504	490	483	506	504	497	501	Si-O bend.	4
460	452	455	460	460	458	458	Si-O-Mg str.	3
420	425	418	420	420	415	420	Si-O-Mg str.	3
–	400	401	–	–	405	–	Si-O-Mg str.	3

str.: stretching; libr: libration; bend.: bending; comb.: combination
References: [1] Farmer (1974); [2] Brindley *et al.* (1979); [3] Parthasarathy *et al.* (2003); [4] Benhammou *et al.* (2009); [5] Tatzber *et al.* (2007).

vibrations of Si–O–Mg bonds (Parthasarathy *et al.*, 2003). All patterns showed the ubiquitous presence of calcite resulting from absorptions at 1790, 1430, 870, and 720 cm^{-1} (Tatzber *et al.*, 2007).

Whole rock. Whole-rock geochemical data (Table 3) indicated that all the clay samples were enriched in Fe_2O_3 (8.52–10.88 wt.%) with respect to MgO (3.79–11.08 wt.%) as well as in some trace elements, such as B (22–132 ppm), Li (11–27 ppm), and Zr (79–221 ppm). The same samples contained large amounts of Sr (229–925 ppm) and Ba (114–557 ppm), which indicate contributions by seawater and/or gabbros. The considerable Ba content (4142 ppm), in particular, in sample CSD 8 was backed up by XRD analyses which indicated the presence of a Ba-rich zeolite (harmotome).

Composition of the hydrocarbons

Macroscopic examination showed that samples CSD 7 and CSD 8 held abundant inclusions of solid, black hydrocarbons (Figure 5), which were picked out using tweezers to prepare KBr pellets for analysis by FTIR. The spectra (Figure 6) exhibited a weak band between 3040 and 3080 cm^{-1} produced by asymmetric stretching vibrations of an aromatic C–H bond (Boukir *et al.*, 1998; Silverstein *et al.*, 2005). The most intense bands were located at 2958 and 2930 cm^{-1}, as well as at 2870 and 2850 cm^{-1}, corresponding to asymmetric and symmetric stretching vibrations of methyl and methylene groups, respectively (Silverstein *et al.*, 2005). The high ratios of intensity I_{2927}/I_{2957} in both samples (0.54 for CSD 7 and 0.95 for CSD 8) suggested the presence of long aliphatic chains (Coelho *et al.*, 2006, and references

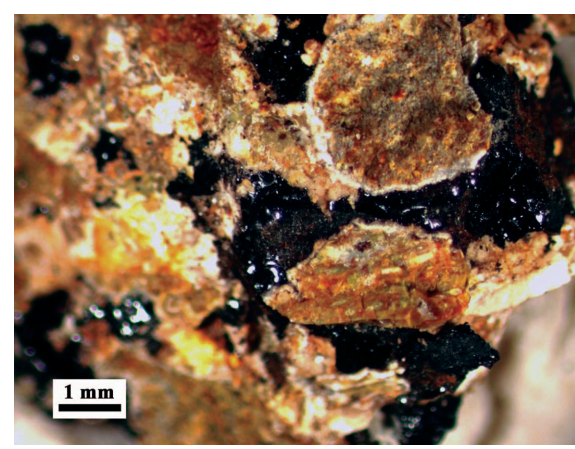

Figure 5. Solid black hydrocarbons in sample CSD 8.

Table 3. Whole-rock geochemical data of S. Demetrio clays, reporting abundances of major (wt.%), minor (ppm), and trace elements (ppm), recalculated on a calcite-free basis.

	CSD 3	CSD 4	CSD 5	CSD 6	CSD 7	CSD 8	CSD 11
SiO_2	52.04	50.98	50.68	52.53	48.02	42.72	47.28
TiO_2	1.99	2.15	1.49	1.86	2.03	2.62	2.17
Al_2O_3	13.68	16.21	12.70	15.07	15.27	12.27	13.52
Fe_2O_3	10.88	9.04	9.31	10.74	8.52	9.57	10.11
MnO	0.02	0.10	0.07	0.06	0.10	0.21	0.10
MgO	3.79	4.33	11.08	3.90	4.07	4.12	5.20
CaO	0.93	2.06	1.27	0.94	1.36	3.36	2.52
Na_2O	0.22	0.17	0.31	0.09	0.16	0.19	0.05
K_2O	4.60	3.97	1.62	4.08	3.74	0.95	2.46
P_2O_5	0.71	1.09	0.96	0.72	1.03	2.55	1.91
L.O.I.	11.14	9.90	10.50	10.02	15.71	21.43	14.69
TOT.	100.00	100.00	100.00	100.00	100.00	100.00	100.00
CaO	0.60	25.80	30.02	4.10	21.10	14.72	5.92
CO_2	0.47	20.25	23.56	3.22	16.56	11.55	4.64
$CaCO_3$	1.07	46.05	53.58	7.32	37.66	26.27	10.56
Li	11	27	19	14	19	11	20
Be	3	–	–	–	2	0.70	–
B	83	22	28	132	102	27	84
S	0.08	–	–	–	0.99	0.82	–
Sc	19.40	–	–	–	12.80	13.40	–
V	139	90	66	117	108	131	347
Cr	179	135	104	155	105	120	133
Co	31	34	24	32	36	83	117
Ni	164	151	116	160	118	103	129
Cu	10	–	–	–	65	54.5	–
Zn	88	52	42	71	41	55	53
As	2	–	–	–	5	8	–
Rb	110	17	15	66	50	21	56
Sr	188	489	320	229	294	925	299
Y	32	16	9	27	21	28.40	32
Zr	218	134	79	180	151	199	221
Nb	0	40	19	45	0	62	64
Mo	–	–	–	–	8	11.50	–
Sb	0.50	–	–	–	0.30	–	–
Cs	1.50	–	–	–	0.90	0.45	–
Ba	114	557	248	142	183	4142	276
La	86	98	27	73	57	107	60
Ce	142	199	99	168	94	223	149
Nd	60	–	–	–	38	–	–
Sm	10.50	–	–	–	6.74	–	–
Eu	3.06	–	–	–	2.05	–	–
Tb	1.20	–	–	–	0.90	1.37	–
Yb	2.52	–	–	–	1.78	2.10	–
Lu	0.35	–	–	–	0.25	0.28	–
Hf	4.30	–	–	–	2.90	0.20	–
Ta	3	–	–	–	3.50	–	–
W	8	–	–	–	–	0.10	–
Pb	6	1	2	1	7	3	2
Th	12	11	0	15	9	9	12
U	3.50	–	–	–	4.40	3.97	–

therein). A broad band in the range 1720–1480 cm^{-1} consisted of weak peaks interpreted as aldehydic C=O stretching, conjugated carbonyl vibrations, stretching modes of aromatic C=C rings, asymmetric stretching of carboxylate groups, asymmetric bending of methyl groups, and scissoring modes of methylene groups (Boukir *et al.*, 1998; Wilt *et al.*, 1998; Silverstein *et al.*, 2005). The symmetric bending vibration of methyl groups generated a peak at 1373 cm^{-1} (Boukir *et al.*, 1998). Finally, a series of bands from 1320 to 1146 cm^{-1} corresponded to bending motions of aromatic C–H rings (Silverstein *et al.*, 2005). The spectrum in Figure 2 of

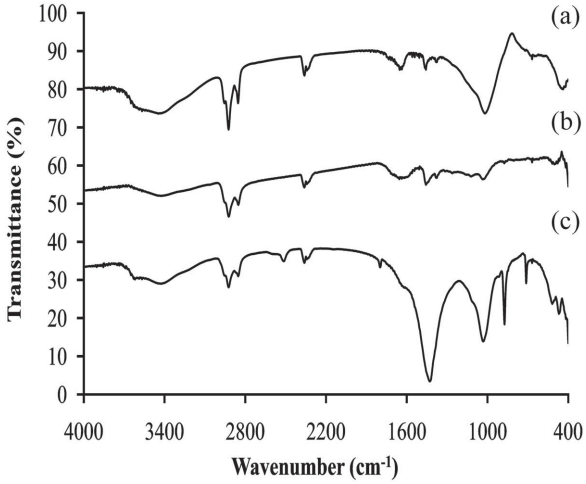

Figure 6. IR spectra of hydrocarbons in samples HT (a) Ciliberto *et al.*, 2009), CSD 8 (b), and CSD 7 (c) in the range 4000–400 cm^{-1}.

sample CSD 7 could be interpreted as a saponite containing aliphatic hydrocarbons, being similar to patterns reported by Flynn *et al.* (2004) in which absorptions near 1600 cm^{-1} and between 1320 and 1146 cm^{-1} were indicative of the aromaticity of the hydrocarbons studied.

DISCUSSION

Origin of the S. Demetrio clays

Mineralogical investigations revealed that all of the clay samples consisted mainly of saponite + carbonates ± quartz ± chrysotile. A similar mineral assemblage was reported in hydrothermal sediments (Nimis *et al.*, 2004; Severmann *et al.*, 2004; Dias and Barriga, 2006; Dekov *et al.*, 2008; Cuadros *et al.*, 2011), derived from mixing of cold seawater and moderately hot hydrothermal fluids (Percival and Ames, 1993), as well as in black shales produced by the weathering of mafic and ultramafic lithologies (Dos Anjos *et al.*, 2010).

Mesozoic black shales and interbedded carbonates were discovered by commercial boreholes in south-eastern Sicily. These lithologies belong to the Noto (Rhaetian) and Streppenosa (Hettangian–Sinermurian) Formations (Bianchi *et al.*, 1987). The clay fraction of these formations (Azzaro *et al.*, 1993) is made up of a mixture of minerals including illite-smectite (I-S), discrete illite, kaolinite, and trace amounts of chlorite-smectite (C-S) and biotite, the smectitic component of which is dioctahedral and of beidellite type. Although some of these clay minerals may be derived from the diagenetic transformation of smectites (Środoń, 1999), the difference in the mineral parageneses of the Streppenosa Formation and the S. Demetrio clays is quite evident, and it rules out a common origin for these sediments, even though making any chemical comparison was impossible because of the lack of geochemical data for the Streppenosa Formation.

In addition, multi-element patterns (Figure 7a,b) of the average composition of S. Demetrio clays, normalized to North American Shale Composite (NASC; Gromet *et al.*, 1984) and non-hydrothermal pelagic sediments (BOFS, Biogeochemical Ocean Flux Study; Cave *et al.*, 2002), highlighted the abundance of P, *REE*, and some transition metals (V, Cr, Fe, Co, Ni, Zn) in the clays studied, which hint at a hydrothermal origin (Dias and Barriga, 2006) for the S. Demetrio clays.

An alternative hypothesis for the origin of the studied clays was considered, with particular reference to their possible formation in a hydrothermal system. Indeed, the occurrence of numerous clayey patches in some Hyblean hydrothermally modified gabbroic xenoliths (Scribano *et al.*, 2006a) led Scribano and Manuella (2008) to infer the presence of a layer of hydrothermal mafic clays, which topped the fossil oceanic core-complex, forming the Hyblean lower crust (Scribano *et al.*, 2006b).The SiO_2/Al_2O_3 *vs.* MgO (wt.%) diagram was used to compare the studied clays with Hyblean hydrothermal smectites (Scribano *et al.*, 2006a; Viccaro *et al.*, 2009), as well as mafic and ultramafic xenoliths (Scribano *et al.*, 2006b; GEOROC database available at http://georoc.mpch-mainz.gwdg.de/georoc/Start.asp). The resulting diagram (Figure 8) showed that S. Demetrio clays overlap the hydrothermal clays and Hyblean

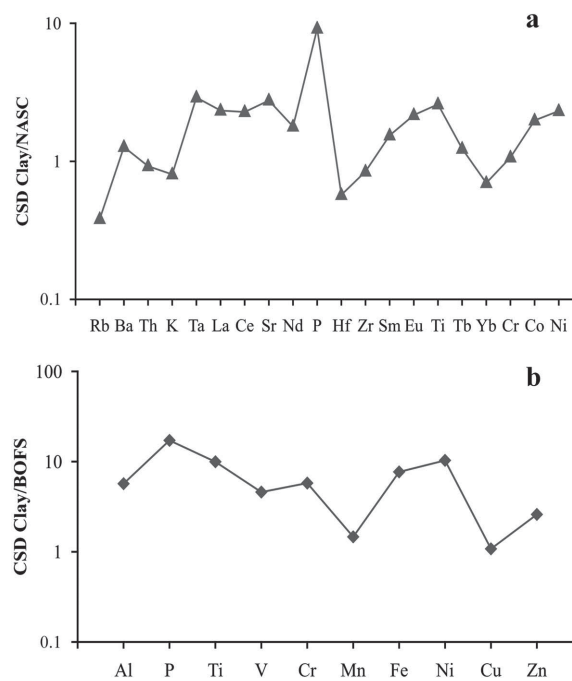

Figure 7. Multi-element pattern of the average composition of S. Demetrio clays, normalized to NASC (North Atlantic Shale composite; Gromet *et al.*, 1984) and BOFS (Biogeochemical Ocean Flux Study; Cave *et al.*, 2002).

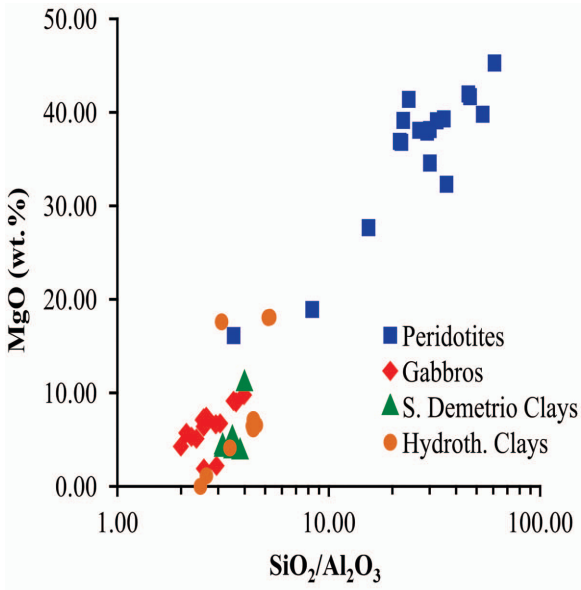

Figure 8. SiO_2/Al_2O_3 *vs.* MgO (wt.%) diagram of S. Demetrio clays, Hyblean hydrothermal clays (Scribano *et al.*, 2006a; Viccaro *et al.*, 2009), Hyblean peridotites, and gabbros (Scribano *et al.*, 2006b; GEOROC database available at http://georoc.mpch-mainz.gwdg.de/georoc/Start.asp).

gabbroic xenoliths. The clays studied showed a strong affinity with sediments derived from oceanic tholeiitic basalts, as demonstrated by the Fe/Ti *vs.* Al/(Al+Fe+Mn) ratio (Figure 9), rather than with those produced by weathering of continental crust rocks (also because kaolinite and dioctahedral Al-rich clay minerals were completely lacking, Dos Anjos *et al.*, 2010).

The evidence above agrees with the reasons which led Sapienza and Scribano (2000) to rule out definitively

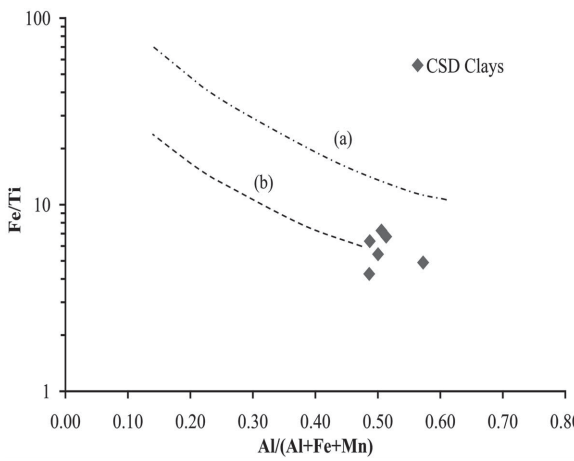

Figure 9. The Fe/Ti *vs.* Al/(Al+Fe+Mn) ratio of S. Demetrio clays (after Boström, 1973). Curve a represents sediments derived from the alteration of continental crust rocks, and curve b is indicative of sediments produced by hydrothermal alteration of oceanic tholeiitic basalts.

the presence of typical continental lithologies (*e.g.* granites, felsic meta-igneous and metasedimentary rocks) in the Hyblean basement, as well as with the lack of contamination by similar rocks in the Hyblean lavas (Trua *et al.*, 1998; Bianchini *et al.*, 1999).

The normalization of the average bulk-rock geochemistry of S. Demetrio clays compared with the average compositions of peridotites and gabbros (Figure 10) highlighted losses of Mg and Na, as well as the loss of some transition metals. On the other hand, S. Demetrio clays contain large amounts of several trace elements, especially *LREE*, compared with NASC (Figure 7), Hyblean peridotites and gabbros (Figure 10).

The mobilization of these elements, particularly *LREE*, could be attributed to the interaction of chloride-rich hydrothermal fluids with the Hyblean mafic and ultramafic rocks (Manuella, 2011), on the basis of field and experimental results (Allen and Seyfried, 2005; Mayanovic *et al.*, 2009; Sansone *et al.*, 2011).

In addition, the plots of B and Li *vs.* SiO_2 and MgO (Figure 11a,b) highlighted a proportional relationship between these elements, which agrees with the experimental results on saponite reported by Vogels *et al.* (2005) which revealed that tetrahedral sheets in phyllosilicates (*i.e.* clay minerals and serpentine) represent the main sinks for B and Li, favored by alkaline conditions (Boschi *et al.*, 2008, and references therein). In particular, the B content in S. Demetrio clays approaches values measured in altered basalts and serpentinized peridotites (Spivack and Edmond, 1987). In fact, recent geochemical investigations on MAR serpentinites (Deschamps *et al.*, 2011) have demonstrated that high concentrations of fluid-mobile elements (FME: Li, Be, B, As, Sb, Pb, U, Ba, Sr, Cs), mobilized by hydrothermal fluids under high seawater/rock ratio and relatively high temperatures (200–300ºC; Schmidt *et al.*, 2011), can be accommodated easily in serpentine minerals. Similarly, the PM-normalized values of fluid-mobile elements reported in Figure 12 show that S. Demetrio clays contain large amounts of FME. This evidence suggests that clay minerals can host FME, similarly to serpentine polytypes, in agreement with experimental results reported by You *et al.* (1996).

Conditions of formation

Some constraints on the physicochemical conditions which pertained during the formation of the observed mineral assemblage can be inferred by the presence of ferric saponite. Generally, saponite precipitates from hydrothermal solutions enriched in silica (a_{SiO_2} = 10^{-6}–10^{-2}; Frost and Beard, 2007) at temperatures ranging from 20 to 150–300ºC (Percival and Ames, 1993; Aoki *et al.*, 1996).

The precipitation of Mg-rich smectites (reaction 1) near hydrothermal vents can be induced by the mixing of cold seawater and hot silica-rich hydrothermal fluids

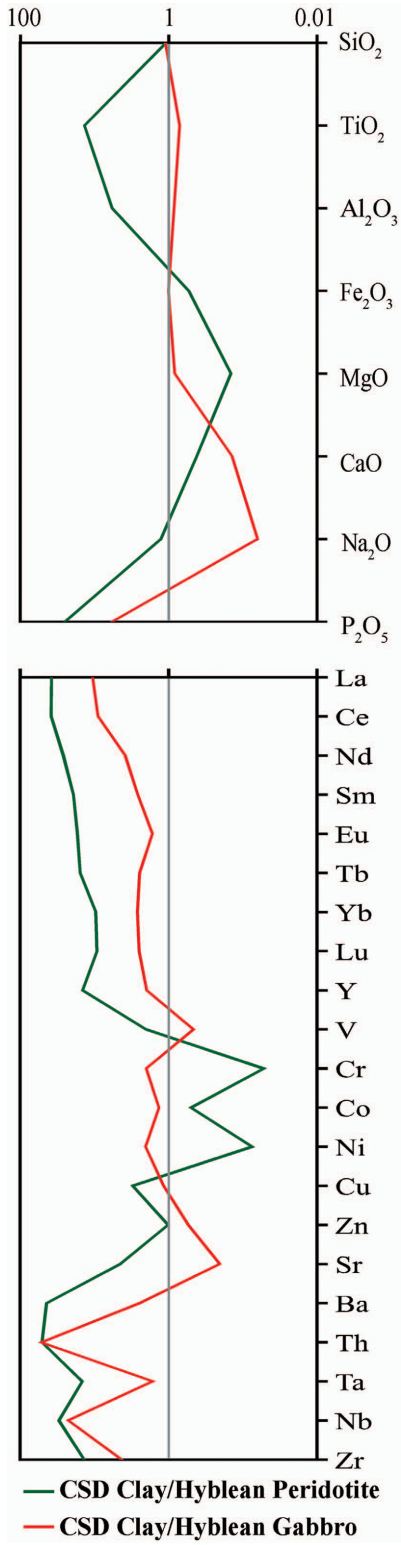

Figure 10. Multi-element patterns of the average composition of S. Demetrio clays normalized to the average compositions of Hyblean peridotites and gabbros (references in the caption of Figure 8).

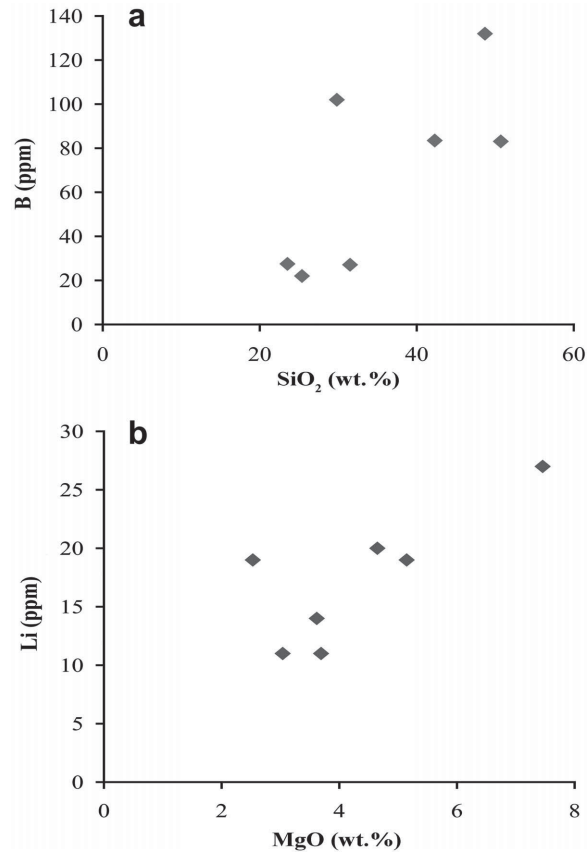

Figure 11. Plots of (a) B (ppm) *vs.* SiO_2 (wt.%) and (b) Li (ppm) *vs.* MgO (wt.%) of S. Demetrio clays.

(Dekov *et al.*, 2008) derived from the interaction of hydrothermal fluids with peridotites and gabbros (Bach *et al.*, 2004, and references therein).

$$6Mg^{2+} + 4OH^{-} + 8SiO_2 + (n+4)H_2O \rightarrow Mg_6Si_8O_{20}(OH)_4{\cdot}nH_2O \text{ (Mg-saponite)} + 8H^{+} \quad (1)$$

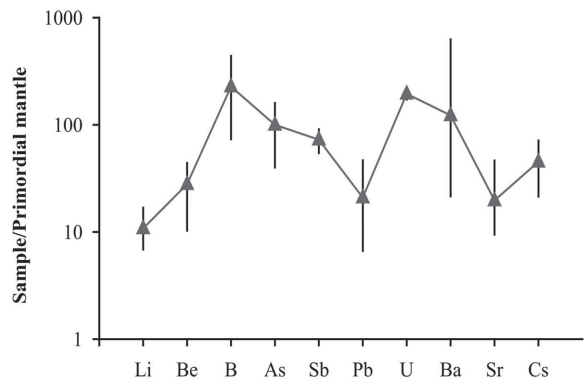

Figure 12. Multi-element pattern of the average concentrations of fluid-mobile elements in S. Demetrio clays, with error bars, normalized to primordial mantle composition (McDonough and Sun, 1995).

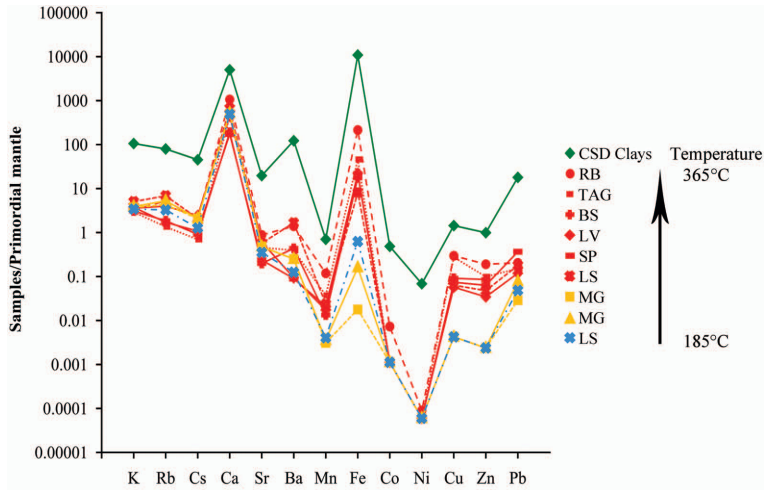

Figure 13. Multi-element patterns of the average compositions of S. Demetrio clays and fluids from some hydrothermal fields (HFs) in MAR (Douville *et al.*, 2002), normalized to primordial mantle composition (McDonough and Sun, 1995).

Several factors, such as temperature, pH, and the Fe/Si ratio of hydrothermal fluids (Kloprogge *et al.*, 1999 and references therein) influence the formation of smectites belonging to the saponite-nontronite solid solution series (Grauby *et al.*, 1994). Cole (1988) noticed that a progressive transformation from saponite (Mg-rich trioctahedral smectite) to nontronite (Fe-rich dioctahedral smectite) occurred, moving away from the hydrothermal vents in Atlantis II Deep (Red Sea), at a decreasing temperature from 160–200 to 80ºC. Indeed, the formation of nontronite in hydrothermal sediments from MAR occurred at low temperature (<100ºC; Severmann *et al.*, 2004; Dias and Barriga, 2006), as inferred by oxygen isotope thermometry.

The presence of Fe-rich saponite in S. Demetrio clays can be attributed to the temperature of fluids which circulated in the fossil ultramafic core complex in the Hyblean lower crust. This temperature was estimated by comparing multi-element distributions (Figure 13) of the average compositions of S. Demetrio clays and fluids from some hydrothermal fields (HFs) in the MAR (Douville *et al.*, 2002), normalized to primordial mantle composition. The comparison shows that the clay pattern resembles those of high-temperature (350–400ºC) hydrothermal fluids from Rainbow and TAG HFs, particularly in relation to the large amounts of some elements (Zr, Nb, Ba, Th, *REE*), consistent with reactions involving gabbroic rocks (Augustin *et al.*, 2008). This inference agrees with the results of mineralogical investigations on some partially serpentinized peridotites from the Hyblean Plateau (Manuella, 2011), which revealed a mineral assemblage (*i.e.* serpentine, sulphides, Na-rich sylvite) suggesting an upper limit of temperature of serpentinization of 350–400ºC.

In addition, the Fe_2O_3/SiO_2 ratio (Figure 14) showed that S. Demetrio clays are related to hydrothermal saponites (Nimis *et al.*, 2004), rather than to hydrothermal nontronites (Severmann *et al.*, 2004; Barrett *et al.*, 1988; Singer *et al.*, 1984). Indeed, trioctahedral to dioctahedral smectites were synthesized under hydrothermal conditions (Mizutani *et al.*, 1991), at a temperature of 100–200ºC, by increasing the Fe/Si ratio. Similar results were obtained by Mosser-Ruck *et al.* (2010), who carried out the experimental conversion of dioctahedral smectites to Fe-rich saponite at T = 300ºC and with a small Fe metal/clay ratio (0.1).

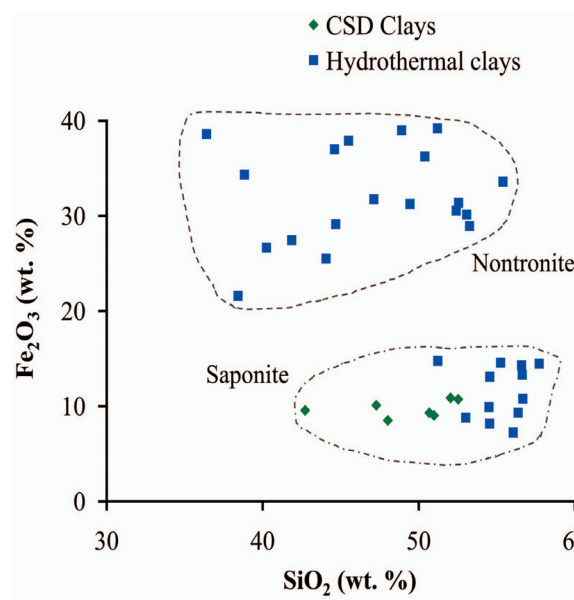

Figure 14. The SiO_2 (wt.%) *vs.* Fe_2O_3 (wt. %) diagram for S. Demetrio clays, with hydrothermal saponite (Nimis *et al.*, 2004) and nontronite (Severmann *et al.*, 2004; Barrett *et al.*, 1988; Singer *et al.*, 1984).

Possible origin of hydrocarbons

The Hyblean Plateau is the location of the most important oil and gas fields in Sicily (Granath and Casero, 2004). Hydrocarbons extracted from there are characterized by large molecular weights (API <20º) and large amounts of S (3−9 wt.%). The only commercial reservoirs of hydrocarbons in southeastern Sicily are found in the Streppenosa-Noto Formations (Granath and Casero, 2004), the clayey and carbonatic fractions of which are the source rocks.

Finding hydrocarbons in some Hyblean metasomatic gabbroic xenoliths (Ciliberto *et al*., 2009) and in highly serpentinized peridotite xenoliths (Scirè *et al.*, 2011) suggests that hydrothermally modified mafic and ultramafic lithologies in the Hyblean lower crust could potentially be reservoir rocks, and probably source rocks also. Indeed, the organic compounds found in Hyblean xenoliths (Scirè *et al.*, 2011; Ciliberto *et al.*, 2009) were probably produced by a Fischer-Tropsch-type (F-T-t) synthesis (reactions 2 and 3) in a serpentinite-hosted hydrothermal system (Scribano *et al.*, 2006a,b).

The abiogenic synthesis of hydrocarbons occurs *via* an exothermic catalytic reduction of CO (F-T-t synthesis) or CO_2 (Sabatier reaction) by gaseous H_2 (reactions 2 and 3), from which some organic compounds found in meteorites, as well as on Earth, could be derived (Taran *et al.*, 2007, and references therein).

$$\text{olivine} + \text{pyroxene} + 3H_2O \rightarrow \text{serpentine} + H_2 \quad (2)$$
$$\Delta H_f^o = -16 \text{ Kcal mol}^{-1} \text{ (MacDonald and Fyfe, 1985)}$$

$$nCO_2 + (3n+1)H_2 \rightarrow C_nH_{(2n+2)} + 2nH_2O \text{ (Konn } et\ al.\text{, 2009)} \quad (3)$$

Serpentinite-hosted hydrothermal systems are ideal loci for the abiogenic production of hydrocarbons *via* F-T-t reaction (Konn *et al.*, 2009), catalyzed by oxides or sulfides of group VIII metals (*e.g.* Fe, Ni, Co; Fu *et al.*, 2007). This reaction caused CO_2 to be reduced to methane and other reduced-carbon phases by H_2 derived from the hydration of primary mafic minerals of peridotites (Marcaillou *et al.*, 2011). Different organic compounds can be produced by F-T-t synthesis, from alkanes and alkenes to heavier hydrocarbons, such as bitumens, waxes, and also crystalline hydrocarbons such as karpatite and idrialite (Szatmari, 1989; Pikovskii *et al.*, 2004). These hydrocarbons are generated by progressive polymerization and polycondensation reactions (Taran *et al.*, 2007) in which the probability of chain growth is expressed by an Anderson-Schulz-Flory (ASF) distribution (Szatmari, 1989). The ASF distribution represents a log-linear relationship of the concentrations of light hydrocarbons and the length of an alkyl chain, possibly indicative of a F-T-t reaction, as well as of thermal degradation of organic matter (Bradley and Summons, 2010).

With regard to the presence of hydrocarbons in the clay samples studied, comparison of the observed absorption bands (Figure 6) in IR spectra with those reported by Ciliberto *et al.* (2009) demonstrated that hydrocarbons are quite similar. Therefore, the association of hydrocarbons with the hydrothermal mineral assemblage studied, the lack of fossil remains, and the affinity of compositions with organic compounds in Hyblean gabbroic xenoliths hint at a possible abiogenic origin for the hydrocarbons hosted in the S. Demetrio clays, even if biogenic or thermogenic mechanisms cannot be ruled out definitively.

Timing of formation of S. Demetrio clays

A final question which must be considered is the dating of the formation of hydrothermal clays in the crustal basement of the Hyblean Plateau. The timing of the hydrothermal system, and hence of serpentinization, was inferred by Scribano *et al.* (2006a) from the age of abundant grains of hydrothermal zircons found in a metasomatitic xenolith, according to Dubińska *et al.* (2004). These minerals were dated to ~246 Ma (Sapienza *et al.*, 2007) using *in situ* U-Pb analyses. Therefore, the timing of formation of hydrothermal clays in the Hyblean basement could have spanned a period from Early to Middle Triassic.

The supposed hydrothermal system could have been active until the first volcanic cycle started in the Hyblean area, during the Late Triassic−Late Cretaceous (Bianchi *et al.*, 1987). After a break of 50 Ma (from the Upper Cretaceous to the Lower Miocene) in igneous activity in the Hyblean region, interaction of an uprising basaltic magma and deep-seated serpentinites, and their alteration products probably occurred, causing the partial breakdown of serpentinites, which can contain up to 250−400 kg m^{-3} of water (Carlson, 2001). The possible release of pressurized fluids ($P_{H_2O} \approx 220$ MPa; Miller *et al.*, 2003) from partially dehydrated serpentinites could be the driving force for the diapiric emplacement of hydrothermal clays at S. Demetrio High, over a time interval from Late Miocene to Early Pleistocene, according to the experimental results of Nermoen *et al.* (2010).

CONCLUSIONS

(1) Clays discovered in the quarry at S. Demetrio High have a mineral assemblage (saponite, calcite, quartz, chrysotile, pyrite, zeolites) and geochemical signatures (abundance of HFSE, Ba, *LREE*, and Eu) which suggest that these minerals were produced by the mixing of high-temperature (350−400ºC) hydrothermal fluids with cold seawater;

(2) The presence of some of the major elements (SiO_2, TiO_2, Al_2O_3, Fe_2O_3) and transition metals (Cr, Co, Ni, Zn) in clays can be attributed to the hydrothermal alteration of mafic and ultramafic lithologies in the Hyblean crustal basement;

(3) Hydrocarbons included in some clay samples show IR absorption bands akin to those observed in

organic compounds in some Hyblean metasomatitic xenoliths (Ciliberto *et al*., 2009), the origin of which can be attributed to a Fischer-Tropsch-type synthesis.

The results here match well with the petrological model proposed by Scribano and Manuella (2008) for the crustal basement of the Hyblean Plateau, suggesting the presence of a hydrothermal clay deposit at the top of the ultramafic core-complex.

ACKNOWLEDGMENTS

This study was supported financially by CARG Project – legge 226/99 – to S. Carbone. The authors are grateful to Prof. R.R. Carrabino for her careful review of the English, and to J.W. Stucki, W.D. Huff, J. Cervini-Silva, and an anonymous reviewer for their constructive review comments.

REFERENCES

Allen, D. and Seyfried, W.E., Jr. (2005) REE controls in ultramafic hosted MOR hydrothermal systems: An experimental study at elevated temperature and pressure. *Geochimica et Cosmochimica Acta*, **69**, 675–683.

Aoki, S., Kohyaman, N., and Hotta, H. (1996) Hydrothermal clay minerals found in sediment containing yellowish-brown material from the Japan Basin. *Marine Geology*, **129**, 331–336.

Augustin, N., Lackschewitz, K.S., Kuhn, T., and Devey, C.W. (2008) Mineralogical and chemical mass changes in mafic and ultramafic rocks from the Logatchev hydrothermal field (MAR 15ºN). *Marine Geology*, **256**, 18–29.

Azzaro, E., Bellanca, A., and Neri, R. (1993) Mineralogy and geochemistry of Mesozoic black shales and interbedded carbonates, southeastern Sicily: evaluation of diagenetic processes. *Geological Magazine*, **130**, 191–202.

Bach, W., Garrido, C.J., Paulick, H., Harvey, J., and Rosner, M. (2004) Seawater-peridotite interactions: First insights from ODP Leg 209, MAR 15ºN. *Geochemistry Geophysics Geosystems*, **5**, 1–22.

Barrett, T.J., Jarvis, I., Longstaffe, F.J., and Farquhar, R. (1988) Geochemical aspects of hydrothermal sediments in the eastern Pacific Ocean: an update. *The Canadian Mineralogist*, **26**, 841–858.

Behncke, B. (1999) Il vulcanesimo del Plateau Ibleo (Sicilia Sud-orientale) negli ultimi 230 Ma. *Bollettino dell'Accademia Gioenia di Scienze Naturali di Catania*, **31**, 39–50.

Ben-Avraham, Z., Boccaletti, M., Cello, G., Grasso, M., Lentini, F., Torelli L., and Tortorici, L. (1990) Principali domini strutturali originatisi dalla collisione neogenico-quaternaria nel Mediterraneo centrale. *Memorie Società Geologica Italiana*, **45**, 453–462.

Benhammou, A., Tanouti, B., Nibou, L., Yaacoubi, A., and Bonnet, J.-P. (2009) Mineralogical and physicochemical investigation of Mg-smectite from Jbel Ghassoul, Morocco. *Clays and Clay Minerals*, **57**, 264–270.

Bianchi, F., Carbone, S., Grasso, M., Invernizzi, G., Lentini, F., Longaretti, G., Merlini, S., and Mostardini, F. (1987) Sicilia orientale: Profilo geologico Nebrodi-Iblei. *Memorie della Società Geologica Italiana*, **38**, 429–458.

Bianchini, G., Bell, K., and Vaccaro, C. (1999) Mantle sources of the Cenozoic Iblean volcanism (SE Sicily, Italy): Sr-Nd-Pb isotopic constraints. *Mineralogy and Petrology*, **67**, 213–222.

Boschi, C., Dini, A., Früh-Green, G.L., and Kelley, D.S. (2008) Isotopic and element exchange during serpentinization and metasomatism at the Atlantis Massif (MAR 30º N): Insights from B and Sr isotope data. *Geochimica et Cosmochimica Acta*, **72**, 1801–1823.

Boukir, A., Guiliano, M., Doumenq, P., El Hallaoui, A., and Mille, G. (1998) Caractérisation structurale d'asphaltènes pétroliers par spectroscopie infrarouge (IRTF). Application à la photo-oxidation. *Comptes Rendus de l'Academie des Sciences de Paris*, **Série II c**, 597–602.

Bradley, A.S. and Summons, R.E. (2010) Multiple origins of methane at the Lost City Hydrothermal Field. *Earth and Planetary Science Letters*, **297**, 34–41.

Brindley, G.W., Bish, D.L., and Wan, H.-M. (1979) Compositions, structures, and properties of nickel-containing minerals in the kerolite-pimelite series. *American Mineralogist*, **64**, 615–625.

Carbone, S. and Lentini, F. (1981) Caratteri deposizionali delle vulcaniti del Miocene superiore negli Iblei (Sicilia Sud-Orientale). *Geologica Romana*, **20**, 79–101.

Carlson, R.L. (2001) The abundance of ultramafic rocks in Atlantic Ocean crust. *Geophysics Journal International*, **144**, 37–48.

Cave, R.R., German, C.R., Thomson, J., and Nesbitt, R.W. (2002) Fluxes to sediments underlying the Rainbow hydrothermal plume at 36º14'N on the Mid-Atlantic Ridge. *Geochimica et Cosmochimica Acta*, **66**, 1905–1923.

Ciliberto, E., Crisafulli, C., Manuella, F.C., Samperi, F., Scirè, S., Scribano, V., Viccaro, M., and Viscuso, E. (2009) Aliphatic hydrocarbons in metasomatized gabbroic xenoliths from Hyblean diatremes (Sicily): genesis in a serpentinite hydrothermal system. *Chemical Geology*, **258**, 258–268.

Coelho, R.R., Hovell, I., de Mello Monte, M.B., Middea, A., and de Souza, A.L. (2006) Characterisation of aliphatic chains in vacuum residues (VRs) of asphaltenes and resins using molecular modelling and FTIR techniques. *Fuel Processing Technology*, **87**, 325–333.

Cole, T.G. (1988) The nature and origin of smectite in the Atlantis II Deep, Red Sea. *The Canadian Mineralogist*, **26**, 755–763.

Cuadros, J., Dekov, V.M., Arroyo, X., and Nieto, F. (2011) Smectite formation in submarine hydrothermal sediments: samples from the HMS Challenger Expedition (1872–1876). *Clays and Clay Minerals*, **59**, 147–164.

Dekov, V.M., Cuadros, J., Shanks, W.C., and Koski, R.A. (2008) Deposition of talc – kerolite-smectite – smectite at seafloor hydrothermal vent fields: evidence from mineralogical, geochemical and oxygen isotope studies. *Chemical Geology*, **247**, 171–194.

Deschamps, F., Guillot, S., Godard, M., Andreani, M., and Hattori, K. (2011) Serpentinites act as sponges for fluid-mobile elements in abyssal and subduction zone environments. *Terra Nova*, **23**, 171–178.

Dias, Á.S. and Barriga, F.J.A.S. (2006) Mineralogy and geochemistry of hydrothermal sediments from the serpentinite-hosted Saldanha hydrothermal field (36º34′N; 33º26′W) at MAR. *Marine Geology*, **225**, 157–175.

Dos Anjos, C.W.D., Meunier, A., Guimaràes, E.M., and El Albani, A. (2010) Saponite-rich black shales and nontronite beds of the Permian Irati Formation: sediment sources and thermal metamorphism (Paraná Basin, Brazil). *Clays and Clay Minerals*, **58**, 606–626.

Douville, E., Charlou, J.-L., Oelkers, E., Bienvenu, H., Jove Colon, P., Donval, F., Fouquet, P., Prieur, Y., and Appriou, D., (2002) The Rainbow vent fluids (36814VN, MAR): the influence of ultramafic rocks and phase separation on trace metal content in Mid-Atlantic Ridge hydrothermal fluids. *Chemical Geology*, **184**, 37–48.

Dubińska, E., Bylina, P., Kozłowski, A., Dörr, W., Nejbert, K., Scastock, J., and Kulicki, C. (2004) U-Pb dating of

serpentinization: hydrothermal zircon from metosomatic rodingite shell (Sudetic Ophiolite, SW Poland). *Chemical Geology*, **203**, 183–203.

Emeis, K.-C. and Weissert, H. (2009) Tethyan–Mediterranean organic carbon-rich sediments from Mesozoic black shales to sapropels. *Sedimentology*, **56**, 247–266.

Farmer, V.C. (1974) The layered silicates. Pp. 331–363 in: *The Infrared Spectra of Minerals* (V.C. Farmer, editor). Monograph **4**, Mineralogical Society, London.

Flynn, G.J., Keller, L.P., Jacobsen, C., and Wirick, S. (2004) An assessment of the amount and types of organic matter contributed to the Earth by interplanetary dust. *Advances in Space Research*, **33**, 57–66.

Frost, B.R. and Beard, J.S. (2007) On silica activity and serpentinization. *Journal of Petrology*, **48**, 1351–1368.

Fu, Q., Sherwood Lollar, B., Horita, J., Lacrampe-Couloume, G., and Seyfried Jr., W.E. (2007) Abiotic formation of hydrocarbons under hydrothermal conditions: constraints from chemical and isotope data. *Geochimica et Cosmochimica Acta*, **71**, 1982–1998.

Gablina, I.F., Semkova, T.A., Stepanova, T.V., and Gor'kova, N.V. (2006) Diagenetic alterations of copper sulfides in modern ore-bearing sediments of the Logatchev-1 hydrothermal field (Mid-Atlantic Ridge 14º45′N). *Lithologies and Mineral Resources*, **41**, 27–44.

Granath, J.W. and Casero, P. (2004) Tectonic setting of the petroleum systems of Sicily. Pp. 391–411 in: *Deformation, Fluid Flow, and Reservoir Appraisal in Foreland Fold and Thrust belts* (R. Swennen, F. Roure, and J.W. Granath, editors). American Association of Petroleum Geologists Hedberg Series, no. 1.

Grasso, M. and Lentini, F. (1982) Sedimentary and tectonic evolution of the eastern Hyblean Plateau (southeastern Sicily) during Late Cretaceous to Quaternary time. *Palaeograohy Palaeoclimatology Palaeoecology*, **39**, 261–280.

Grasso, M., Pedley, H.M., Behncke, B., Maniscalco, R., and Sturiale, G. (2004) Integrated stratigraphic approch to the study of the Neogene-Quaternary sedimentation and volcanism in the northern Hyblean Plateau (Sicily). Pp. 159–166 in: *Mapping Geology in Italy* (G. Pasquarè and C. Venturini, editors), APAT, Rome.

Grauby, O., Petit, S., Decarreau, A., and Baronnet, A. (1994) The nontronite-saponite series: an experimental approach. *European Journal of Mineralogy*, **6**, 99–112.

Gromet, L.P., Dymek, R.F., Haskin, L.A., and Korotev, R.L. (1984) The "North American shale composite": its compilation, major and trace element characteristics. *Geochimica et Cosmochimica Acta*, **48**, 2469–2482.

Kloprogge, J.T., Komarneni, S., and Amonette, J.E. (1999) Synthesis of smectite clay minerals: a critical review. *Clays and Clay Minerals*, **47**, 529–554.

Konn, C., Charlou, J.L., Donval, J.P., Holm, N.G., Dehairs, F., and Bouillon, S. (2009) Hydrocarbons and oxidized organic compounds in hydrothermal fluids from Rainbow and Lost City ultramafic-hosted vents. *Chemical Geology*, **258**, 299–314.

Macdonald, A.H. and Fyfe, W.S. (1985) Rate of serpentinization in seafloor environments. *Tectonophysics*, **116**, 123–135.

Manuella, F.C. (2011) Vein mineral assemblage in partially serpentinized peridotite xenoliths from Hyblean Plateau (South-eastern Sicily, Italy). *Periodico di Mineralogia*, **80**, 247–266.

Marcaillou, C., Muñoz, M., Vidal, O., Parra, T., and Harfouche, M. (2011) Mineralogical evidence for H_2 degassing during serpentinization at 300ºC/300 bar. *Earth and Planetary Science Letters*, **303**, 281–290.

Mayanovic, R.A., Anderson, A.J., Bassett, W.A., and Chou, I.M. (2009) Steric hindrance and the enhanced stability of light rare-earth elements in hydrothermal fluids. *American Mineralogist*, **94**, 1487–1490.

McDonough, W.F. and Sun, S.-s. (1995) The composition of the Earth. *Chemical Geology*, **120**, 223–253.

Miller, S.A., van der Zee, W., Olgaard, D.L., and Connolly, J.A.D. (2003) A fluid-pressure feedback model of dehydration reactions: experiments, modelling, and application to subduction zones. *Tectonophysics*, **370**, 241–251.

Mizutani, T., Fukushima, Y., Doi, H., and Kamigaito, O. (1991) Process for producing clay mineral of chain structure. *United States Patent*, **no. 4987106**, 1–6.

Mosser-Ruck, R., Cathelineau, M., Guillaume, D., Charpentier, D., Rousset, D., Barres, O., and Michau, N. (2010) Effects of temperature, pH, and iron/clay and liquid/clay ratios on experimental conversion of dioctahedral smectites to berthierine, chlorite, vermiculite, or saponite. *Clays and Clay Minerals*, **58**, 280–291.

Nermoen, A., Galland, O., Jettestuen, E., Fristad, K., Podladchikov, Y., Svensen, H., and Malthe-Sørenssen, A. (2010) Experimental and analytic modeling of piercement structures. *Journal of Geophysical Research*, **115**, B10202, doi:10.1029/2010JB007583.

Nimis, P., Tesalina, S.G., Omenetto, P., Tartarotti, P., and Lerouge, C. (2004) Phyllosilicate minerals in the hydrothermal mafic–ultramafic-hosted massive-sulfide deposit of Ivanovka (southern Urals): comparison with modern ocean seafloor analogues. *Contributions to Mineralogy and Petrology*, **147**, 363–383.

Parthasarathy, G., Choudary, B.M., Sreedhar, B., Kunwar, A.C., and Srinivasan, R. (2003) Ferrous saponite from the Deccan Trap, India, and its application in adsorption and reduction of hexavalent chromium. *American Mineralogist*, **88**, 1983–1988.

Percival, J.B. and Ames, D.E. (1993) Clay mineralogy of active hydrothermal chimneys and an associated mound, Middle Valley, Northern Juan de Fuca Ridge. *The Canadian Mineralogist*, **31**, 957–971.

Pikovskii, Y.L., Chernova, T.G., Alekseeva, T.A., and Verkhovskaya, Z.I. (2004) Composition and nature of hydrocarbons in modern serpentinization areas in the ocean. *Geochemistry International*, **42**, 971–976.

Sansone, M.T.C., Rizzo, G., and Mongelli, G. (2011) Petrochemical characterization of mafic rocks from the Ligurian ophiolites, southern Apennines. *International Geology Review*, **53**, 130–156.

Sapienza, G. and Scribano, V. (2000) Distribution and representative whole-rock chemistry of deep-seated xenoliths from the Iblean Plateau, south-eastern Sicily, Italy. *Periodico di Mineralogia*, **69**, 185–204.

Sapienza, G., Griffin, W.L., O'Reilly, S.Y., and Morten, L. (2007) Crustal zircons and mantle sulfides: Archean to Triassic events in the lithosphere beneath south-eastern Sicily. *Lithos*, **96**, 503–523.

Scarascia, S., Cassinis, R., Lozej, A., and Nebuloni, A. (2000) A seismic and gravimetric model of crustal structures across the Sicily Channel Rift Zone. *Bollettino della Società Geologica Italiana*, **19**, 213–222.

Schmidt, K., Garbe-Schönberg, M., Koschinsky, A., Strauss, H., Jost, C.L., Klevenz, V., and Köninger, P. (2011) Fluid elemental and stable isotope composition of the Nibelungen hydrothermal field (8º18'S, Mid-Atlantic Ridge): constraints on fluid–rock interaction in heterogeneous lithosphere. *Chemical Geology*, **280**, 1–18.

Scirè, S., Ciliberto, E., Crisafulli, C., Scribano, V., Bellatreccia, F., and Della Ventura, G. (2011) Asphaltene-bearing mantle xenoliths from Hyblean diatremes, Sicily. *Lithos*, **125**, 956–968.

Scribano, V. (1986) The harzburgite xenoliths in a Quaternary

basanitoid lava near Scordia (Hyblean plateau, Sicily). *Rendiconti della Società Italiana di Mineralogia e Petrologia*, **41**, 245–255.

Scribano, V. (1987) The ultramafic and mafic nodule suite in a tuff-breccia pipe from Cozzo Molino (Hyblean Plateau, SE Sicily). *Rendiconti della Società Italiana di Mineralogia e Petrologia*, **42**, 203–217.

Scribano, V. and Manuella, F.C. (2008) Early seafloor exposure of Hyblean uppermost mantle and prime role of serpentinization for plateau uplifting: a xenolith perspective. *Atti del Congresso 'Tethys to Mediterranean: a journey of geological discovery'*, Catania 3–5 June 2008, p. 103.

Scribano, V., Ioppolo, S., and Censi, P. (2006a) Chlorite/smectite-alkali feldspar metasomatica xenoliths from Hyblean Miocenic diatremes (Sicily, Italy): evidence for early interaction between hydrothermal brines and ultramafic/mafic rocks at crustal levels. *Ofioliti*, **31**, 161–171.

Scribano, V., Sapienza, G.T., Braga, R., and Morten, L. (2006b) Gabbroic xenoliths in tuff-breccia pipes from the Hyblean Plateau: insights into the nature and composition of the lower crust underneath South-eastern Sicily, Italy. *Mineralogy and Petrology*, **86**, 63–88.

Severmann, S., Mills, R.A., Palmer, M.R., and Fallick, A.E. (2004) The origin of clay minerals in active and relict hydrothermal deposits. *Geochimica et Cosmochimica Acta*, **68**, 73–88.

Silverstein, R.M., Webster, F.X., and Kiemle, D.J. (2005) *Spectroscopic Identification of Organic Compounds*, 7th edition. John Wiley and Sons, New Jersey, USA.

Singer, A., Stoffers, P., Heller-Kallai, L., and Szafranek, D. (1984) Nontronite in deep-sea core from the south Pacific. *Clays and Clay Minerals*, **32**, 375–383.

Spivack, A.J. and Edmond, J.M. (1987) Boron isotope exchange between seawater and the oceanic crust. *Geochimica et Cosmochimica Acta*, **51**, 1033–1043.

Środoń, J. (1999) Nature of mixed-layer clays and mechanisms of their formation and alteration. *Annual Review in Earth and Planetary Sciences*, **27**, 19–53.

Szatmari, P. (1989) Petroleum formation by Fischer-Tropsch synthesis in plate tectonics. *AAPG Bulletin*, **73**, 989–998.

Taran, Y.A., Kliger, G.A., and Sevastianov, V.S. (2007) Carbon isotope effects in the open-system Fischer–Tropsch synthesis. *Geochimica et Cosmochimica Acta*, **71**, 4474–4487.

Tatzber, M., Stemmer, M., Spiegel, H., Katzlberger, C., Haberhauer, G., and Gerzabek, M.H. (2007) An alternative method to measure carbonate in soils by FTIR spectroscopy. *Environmental Chemistry Letters*, **5**, 9–12.

Torelli, L., Grasso, M., Mazzoldi, G., and Peis, D. (1998) Plio-Quaternary tectonic evolution and structure of the Catania foredeep, the northern Hyblean Plateau and the Ionian shelf (SE Sicily). *Tectonophysics*, **298**, 209–221.

Trua, T., Laurenzi, M.A., and Oddone, M. (1997) Geochronology of the Plio-Pleistocene Hyblean volcanism (SE Sicily): new $^{40}Ar/^{39}Ar$ data. *Acta Vulcanologica*, **9**, 167–176.

Trua, T., Esperança, S., and Mazzuoli, R. (1998) The evolution of the lithospheric mantle along the N. African plate: geochemical and isotopic evidence from the tholeiitic and alkaline volcanic rocks of the Hyblean Plateau, Italy. *Contributions to Mineralogy and Petrology*, **131**, 307–322.

Viccaro, M., Scribano, V., Cristofolini, R., Ottolini, L., and Manuella, F.C. (2009) Primary origin of some trachytoid magmas: Inferences from naturally quenched glasses in hydrothermally metasomatized gabbroic xenoliths (Hyblean area, Sicily). *Lithos*, **113**, 659–672.

Vogels, R.J.M.J., Kloprogge, J.T., and Geus, J.W. (2005) Synthesis and characterisation of boron and gallium substituted saponite clays below 100ºC at one atmosphere. *Microporous and Mesoporous Materials*, **77**, 159–165.

Wilt, B.K., Welch, W.T., and Rankin, J.G. (1998) Determination of asphaltenes in petroleum crude oils by Fourier Transform Infrared Spectroscopy. *Energy and Fuels*, **12**, 1008–1012.

You, C.-F., Castillo, P.R., Gieskes, J.M., Chan, L.H., and Spivack, A.J. (1996) Trace element behavior in hydrothermal experiments: Implications for fluid processes at shallow depths in subduction zones. *Earth and Planetary Science Letters*, **140**, 41–52.

Zappaterra, E. (1994) Source-rock distribution model of the Periadriatic Region. *American Association of Petroleum Geologists Bulletin*, **78**, 333–354.

(*Received 9 May 2011; revised 29 December 2011; Ms. 568; A.E. W. Huff*)